Pro-BDNF–induced synaptic depression and retraction at developing neuromuscular synapses

Feng Yang,[1,2] Hyun-Soo Je,[1,2] Yuanyuan Ji,[1,2] Guhan Nagappan,[1,2] Barbara Hempstead,[3] and Bai Lu[1,2]

[1]Section on Neural Development and Plasticity, National Institute of Child Health and Human Development and [2]Genes, Cognition, and Psychosis Program, National Institute of Mental Health, National Institutes of Health, Bethesda, MD 20892
[3]Division of Hematology and Medical Oncology, Department of Medicine, Weill Cornell Medical College of Cornell University, New York, NY 10021

Postsynaptic cells generate positive and negative signals that retrogradely modulate presynaptic function. At developing neuromuscular synapses, prolonged stimulation of muscle cells induces sustained synaptic depression. We provide evidence that pro–brain-derived neurotrophic factor (BDNF) is a negative retrograde signal that can be converted into a positive signal by metalloproteases at the synaptic junctions. Application of pro-BDNF induces a dramatic decrease in synaptic efficacy followed by a retraction of presynaptic terminals, and these effects are mediated by presynaptic pan-neurotrophin receptor p75 (p75^{NTR}), the pro-BDNF receptor. A brief stimulation of myocytes expressing cleavable or uncleavable pro-BDNF elicits synaptic potentiation or depression, respectively. Extracellular application of metalloprotease inhibitors, which inhibits the cleavage of endogenous pro-BDNF, facilitates the muscle stimulation–induced synaptic depression. Inhibition of presynaptic p75^{NTR} or postsynaptic BDNF expression also blocks the activity-dependent synaptic depression and retraction. These results support a model in which postsynaptic secretion of a single molecule, pro-BDNF, may stabilize or eliminate presynaptic terminals depending on its proteolytic conversion at the synapses.

Introduction

The nervous system responds to experience by altering the number and strength of synaptic connections (Katz and Shatz, 1996). Activity-dependent synaptic stabilization and elimination play a critical role in shaping patterns of neuronal connections during brain development (Constantine-Paton et al., 1990; Lichtman and Colman, 2000; Debski and Cline, 2002; Goda and Davis, 2003; Hensch, 2005; Taha and Stryker, 2005). Although the molecular mechanisms by which neuronal activity alters synaptic connectivity remains largely unknown, it is believed that postsynaptic cells often generate positive and negative signals that retrogradely alter presynaptic structure and function (Balice-Gordon et al., 1993; Lo et al., 1994).

Using *Xenopus laevis* nerve–muscle coculture as a model system, Lo et al. (1994) and Cash et al. (1996) elegantly demonstrated that postsynaptic activity is critical for synaptic depression, a process which may be important for proper development of neuronal circuits. For example, prolonged postsynaptic stimulation of myocytes results in a significant and sustained reduction in synaptic efficacy (Dan and Poo, 1992; Lo and Poo, 1994; Lo et al., 1994). Inhibition of postsynaptic Ca^{2+} rise by the Ca buffer BAPTA prevents synaptic depression, whereas an increase in cytosolic Ca^{2+} by photo-uncaging in the postsynaptic myocytes is sufficient to induce persistent synaptic depression (Cash et al., 1996). These results suggest that postsynaptic Ca^{2+} signaling is important for the release of a retrograde factor, which in turn acts on presynaptic terminals to induce synaptic depression (Dan et al., 1995; Poo, 2001). Furthermore, a brief presynaptic stimulation induces synaptic potentiation, which is also dependent on postsynaptic Ca^{2+} and retrograde signaling (Wan and Poo, 1999). However, the nature of the retrograde factor has not been established.

Neurotrophins have been recognized as key regulators of synapse development and plasticity (Poo, 2001; Lu, 2003). One such factor, brain-derived neurotrophic factor (BDNF), elicits a rapid increase in transmitter release by activating presynaptic

F. Yang and H.-S. Je contributed equally to this paper.

Correspondence to Bai Lu: bailu@mail.nih.gov

Abbreviations used in this paper: α-BTX, α-bungarotoxin; AChR, acetylcholine receptor; BDNF, brain-derived neurotrophic factor; CNS, central nervous system; COM, center of mass; ESC, evoked synaptic current; LTP, long-term potentiation; mBDNF, mature BDNF; MMP, matrix metalloprotease; NMJ, neuromuscular junction; p75^{NTR}, pan-neurotrophin receptor p75; ROI, region of interest; SSC, spontaneous synaptic current; Trk, tropomyosin-related kinase.

The Rockefeller University Press $30.00
J. Cell Biol. Vol. 185 No. 4 727–741
www.jcb.org/cgi/doi/10.1083/jcb.200811147

tropomyosin-related kinase (Trk) B receptors when applied acutely to the neuromuscular synapses (Lohof et al., 1993). In addition, long-term BDNF treatment promotes synapse maturation (Wang et al., 1995). Similar to other neurotrophins, BDNF is initially synthesized as a precursor (pro-BDNF), which is subsequently cleaved to generate mature BDNF (mBDNF). Pro-BDNF interacts preferentially with the pan-neurotrophin receptor p75 ($p75^{NTR}$), whereas mBDNF selectively binds and activates the receptor Tyr kinase TrkB (Chao and Bothwell, 2002; Ibanez, 2002). Cumulative evidence supports a "yin-yang" hypothesis, in which pro- and mBDNF elicit opposite biological effects by activating two distinct receptor systems (Lu et al., 2005). For example, activation of $p75^{NTR}$, most likely by endogenous pro-BDNF, appears to be critical for long-term depression in the hippocampus (Rosch et al., 2005; Woo et al., 2005). In contrast, mBDNF-TrkB signaling is essential for the early phase of long-term potentiation (LTP; Korte et al., 1995; Figurov et al., 1996; Patterson et al., 1996). Although the secretion of pro-BDNF was initially questioned (Matsumoto et al., 2008), substantial evidence now demonstrates that a significant proportion of BDNF in the brain is secreted in the pro form (Teng et al., 2005; Nagappan et al., 2009; Yang et al., 2009). Moreover, extracellular conversion of pro-BDNF to mBDNF by the tissue plasminogen activator/plasmin protease system is critical for late-phase LTP (Pang et al., 2004). The expression of pro-BDNF and $p75^{NTR}$ in rodents is developmentally regulated, with the highest levels in the first and second postnatal week, correlating well with synapse formation and elimination (Yang et al., 2009). In this study, we sought to test the hypothesis that pro-BDNF is a retrograde signal that induces synaptic depression after postsynaptic stimulation at the neuromuscular synapse. We demonstrate that exogenous pro-BDNF suppresses synaptic transmission and structurally causes axonal retraction by activating presynaptic $p75^{NTR}$. We provide evidence that muscle stimulation induces secretion of pro-BDNF, which elicits either synaptic potentiation or depression depending on whether it is proteolytically cleaved. Metalloproteases appear to be a major class of proteases mediating pro-BDNF to mBDNF conversion at the neuromuscular junction (NMJ). These findings provide mechanistic insight into how positive and negative signals could be derived from the same molecule and suggest that proteolytic cleavage of pro-BDNF is an important regulatory step in BDNF signaling and synapse refinement.

Results

Expression of TrkB, $p75^{NTR}$, and pro-BDNF at *Xenopus* neuromuscular synapses

Xenopus nerve–muscle coculture is a well suited system to study activity-dependent synaptic modulation and synaptic actions of neurotrophins (Lo and Poo, 1991, 1994; Lohof et al., 1993; Lo et al., 1994; Wang et al., 1995; Je et al., 2006). In this system, mBDNF elicits an acute effect on synaptic transmission and long-term effects on synapse maturation through the activation of presynaptic TrkB (Lohof et al., 1993; Wang et al., 1995). Consistent with this, we detected strong TrkB immunoreactivity in presynaptic neurons as well as at the NMJ in culture (Fig. S1 A). A previous study indicated that spinal motor neurons express a high level of $p75^{NTR}$ during early development, but its expression subsides after the formation of NMJs postnatally (Yan and Johnson, 1988). Indeed, $p75^{NTR}$ was strongly expressed in the developing spinal neurons, particularly at the presynaptic terminals that innervated the myocytes (Fig. S1 B). We next examined the expression and secretion of pro-BDNF, the ligand for $p75^{NTR}$. In *Xenopus* nerve–muscle cultures, immunofluorescence staining under membrane permeable conditions detected pro-BDNF in postsynaptic muscle cells but not at the presynaptic terminals (Fig. S1 C). Western blot analysis revealed the expression of pro-BDNF in muscle tissues in vivo in various stages of *Xenopus* development (Fig. S1 D).

Synaptic depression induced by exogenous pro-BDNF

To determine the functional role of pro-BDNF, we applied a recombinant, cleavage-resistant pro-BDNF (Woo et al., 2005) to *Xenopus* nerve–muscle cocultures. Spontaneous synaptic currents (SSCs) and impulse-evoked synaptic currents (ESCs) were monitored using whole-cell voltage clamp (Yang et al., 2001). The application of 2 ng/ml pro-BDNF markedly inhibited spontaneous synaptic transmission recorded in the presence of 1 μM tetrodotoxin (Fig. 1 A). The mean SSC frequency was 11.8 ± 1.2 events/min before pro-BDNF application, but it decreased to 2.9 ± 0.4 events/min 40 min after pro-BDNF application ($P < 0.001$; *t* test). This decrease in synaptic efficacy is not caused by a toxic side effect of pro-BDNF because the treatment of the cultures with pro-BDNF for >24 h did not induce obvious apoptosis of the spinal neurons or myocytes (Fig. S1 E). Furthermore, pro-BDNF–mediated synaptic depression was recovered after washing out pro-BDNF within 5–10 min (Fig. 1, A and B), which argued against an apoptotic effect of pro-BDNF. In addition to the SSC frequency, the application of pro-BDNF markedly reduced SSC amplitude ($P < 0.02$; Fig. 1 C). Several experiments were performed to determine the underlying mechanisms by which pro-BDNF elicits synaptic depression. The kinetics of FM dye destaining was the same in control and pro-BDNF–treated groups (Fig. S2), suggesting that the probability of presynaptic transmitter release is not altered by pro-BDNF treatment. Moreover, acetylcholine receptor (AChR) clusters, labeled by a low concentration of rhodamine-conjugated α-bungarotoxin (α-BTX; 100 nM), were not dispersed after pro-BDNF treatment, even after axonal retraction had occurred (Fig. S3). Thus, postsynaptic dispersion of AChRs was not the cause for synaptic depression. Finally, the analysis of SSC kinetics revealed that pro-BDNF increased both the rise and decay times of SSCs (Fig. 1 D). This result, together with the dramatic decrease in SSC frequency induced by pro-BDNF, supports the notion that the distance between pre- and postsynaptic membranes might become wider. However, we cannot completely rule out the possibility that pro-BDNF may induce a switch of transmitter release from synaptic to extrasynaptic site.

To determine the role of pro-BDNF in functional synaptic transmission, we measured the amplitude of ESCs elicited by stimulating presynaptic somata of spinal neurons (Yang et al., 2001). Application of pro-BDNF dramatically reduced ESC

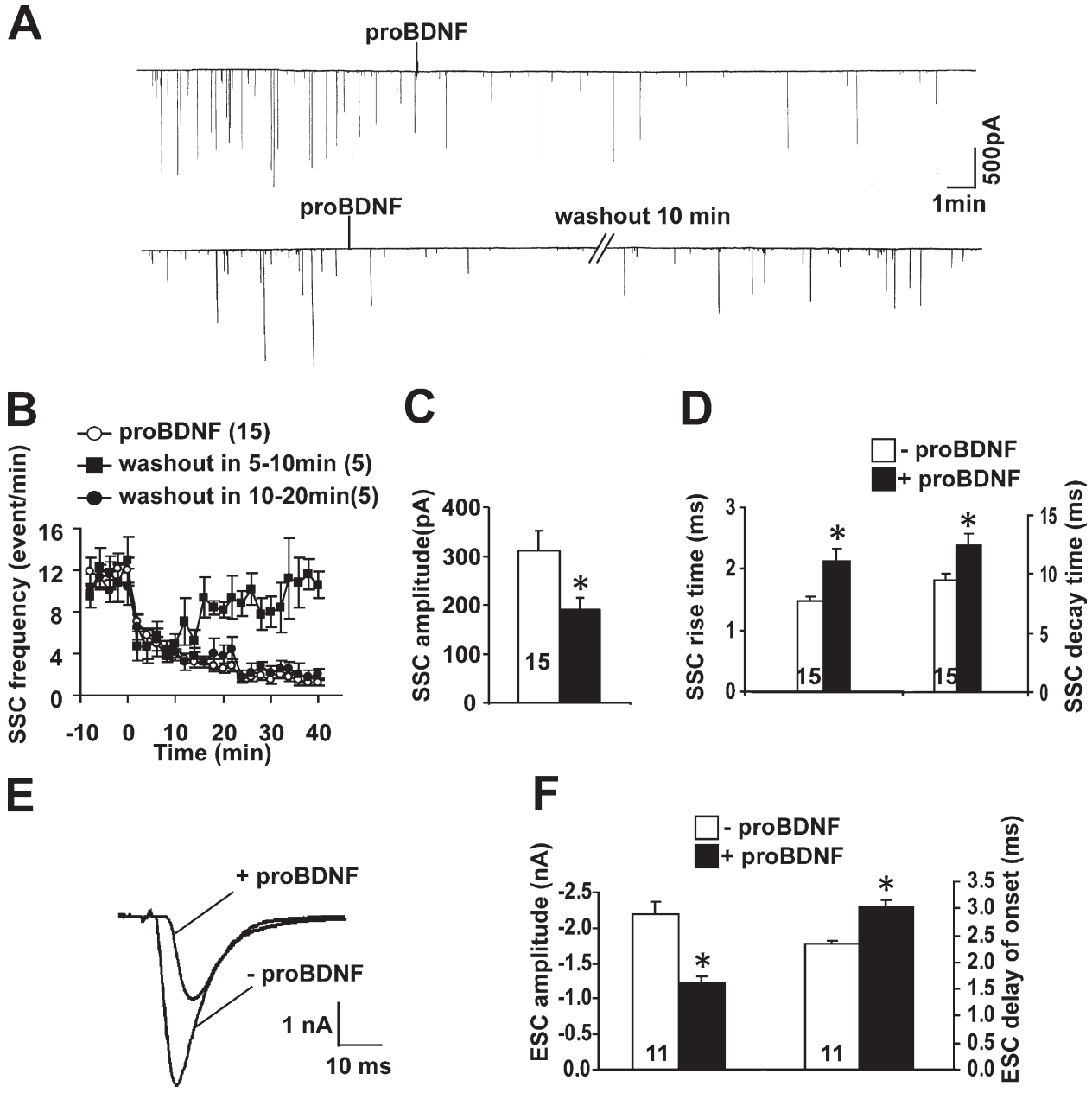

Figure 1. **Synaptic depression induced by pro-BDNF application.** Data from individual synapses were averaged from 10 min of recording before and 30 min after pro-BDNF treatment. All data are presented as mean ± SEM. The number associated with each bar in the graphs represents the number of cells analyzed. The asterisks indicate a significantly higher result than that for the respective "before treatment" group by a *t* test (*, $P < 0.05$). (A) Sample recordings of SSCs from a neuromuscular synapse before and after the application of cleavage-resistant pro-BDNF. The top recording shows a rapid and persistent decrease in SSC frequency after pro-BDNF application, whereas the bottom recording demonstrates the recovery of synaptic efficacy after washout of pro-BDNF from the culture. (B) Time course of pro-BDNF–induced synaptic depression. Each point represents the mean frequency of SSCs (every 2 min) for 10 min before and 40 min after pro-BDNF treatment. After washout of pro-BDNF from culture within 5–10 min (closed square), the synaptic efficacy was recovered. However, after pro-BDNF washout after 10 min (closed circle), the synaptic depression persisted. The numbers in parentheses indicate the number of synapses recorded. (C) Effect of pro-BDNF on SSC amplitude. (D) Effect of pro-BDNF on rise time and decay time of SSCs. (E) Superimposed traces of ESCs before and 30 min after pro-BDNF treatment. (F) Amplitude and delay of onset of ESCs before and after pro-BDNF treatment.

amplitude (Fig. 1, E and F). The amplitude was 2,182 ± 196 pA in control but 1,228 ± 92 pA 10 min after pro-BDNF treatment ($P < 0.0001$). Moreover, pro-BDNF significantly increased the delay of onset (Fig. 1 F), which also indicated the widening of synaptic clefts. Collectively, these results suggested that pro-BDNF may cause the physical retraction of presynaptic terminals from postsynaptic muscle cells rather than a suppression of synaptic transmission by modifying either pre- or postsynaptic elements.

Pro-BDNF–induced synaptic depression is mediated by $p75^{NTR}$

To determine whether pro-BDNF induces synaptic retraction by activating $p75^{NTR}$, we designed an siRNA against both *Xenopus p75NTRa* and *p75NTRb* genes (Hutson and Bothwell, 2001). The embryo injection at the two-cell stage was used to introduce the siRNA into either neurons or myocytes (see Materials and methods; Yang et al., 2001). Western blot analysis revealed

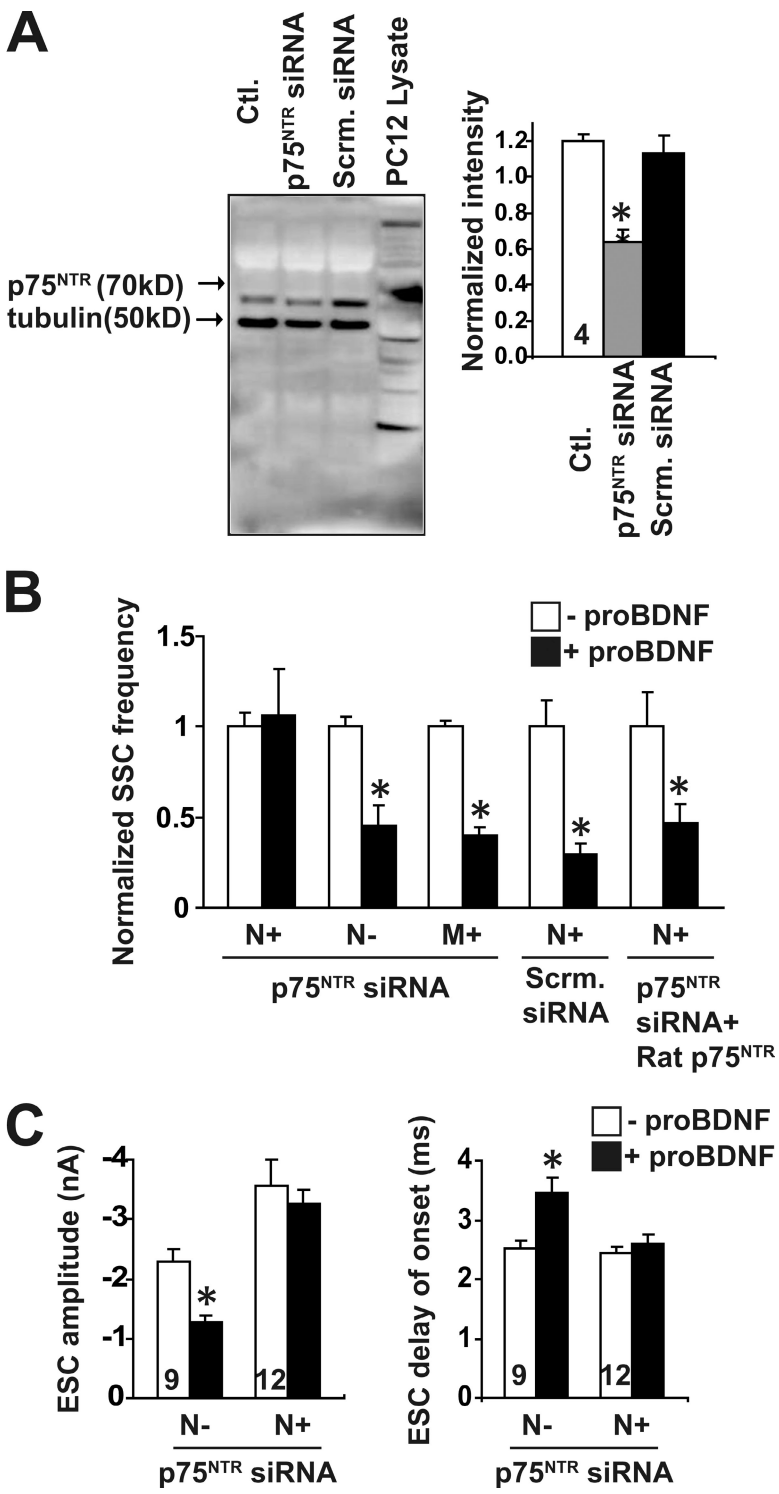

Figure 2. **Pro-BDNF–mediated synaptic depression is mediated by presynaptic p75^{NTR}.** (A) Down-regulation of p75^{NTR} by siRNA. p75^{NTR}-specific siRNA and scrambled (Scrm.) analogues were introduced into the developing *Xenopus* by embryo injection. Neural tubes were dissected, and proteins were extracted. Western blots were performed using anti-p75^{NTR}–specific antibody together with an antitubulin antibody for loading controls. Note a reduction of p75^{NTR} expression in p75^{NTR} siRNA–injected but not in uninjected (control [Ctl.]) or scrambled siRNA–injected embryos (left). Quantitative analysis of p75^{NTR} expression in four independent experiments (right) is shown. The number in the bar indicates the number of Western blots performed. (B) Attenuation of pro-BDNF effect on SSCs by presynaptic expression of siRNA and its rescue by coexpression with rat p75^{NTR}. p75^{NTR} siRNA was expressed in presynaptic neurons (N+), postsynaptic myocytes (M+), or not at all (N−). Scrambled p75^{NTR} siRNA was used as a control. In the last set of experiments, coexpression of p75^{NTR} siRNA with rat p75^{NTR} mRNA reversed the effect of p75^{NTR} siRNA. (C) Effect of p75^{NTR} siRNA on pro-BDNF–induced depression of ESCs. Amplitude (left) and delay of onset (right) of ESCs at control synapses (N−) and synapses expressing p75^{NTR} siRNA (N+) are presented. The numbers in the bars indicate the number of synapses recorded. (A–C) Error bars represent SEM. *, $P < 0.05$.

an ∼40% reduction of endogenous p75^{NTR} in homogenates of neural tubes derived from embryos injected with p75^{NTR} siRNA (Fig. 2 A). Because only a fraction of the cells in the injected embryos received p75^{NTR} siRNA, the actual down-regulation of p75^{NTR} in an individual cell, which contains siRNA, should be far more pronounced. As a control, injection of scrambled siRNA into the embryos failed to down-regulate p75^{NTR} expression (Fig. 2 A). The injected embryos were used to prepare nerve–muscle cocultures in which the p75^{NTR} siRNA was selectively expressed in either presynaptic spinal neurons or postsynaptic muscle cells, as indicated by coexpressed GFP. Neuronal expression of p75^{NTR} siRNA but not scrambled siRNA prevented pro-BDNF–induced synaptic depression (Fig. 2 B). However, the expression of p75^{NTR} siRNA in postsynaptic muscle cells did not prevent pro-BDNF–induced synaptic depression (Fig. 2 B). To confirm the specificity of p75^{NTR} siRNA, we performed rescue experiments by coexpressing p75^{NTR} siRNA with rat p75^{NTR} mRNA in presynaptic neurons because nucleotide

sequences corresponding to the siRNA against *Xenopus* $p75^{NTR}$ were not found in the rat $p75^{NTR}$ homologue. Neurons expressing both $p75^{NTR}$ siRNA and rat $p75^{NTR}$ mRNA exhibited pro-BDNF–induced synaptic depression, indicating the specificity of $p75^{NTR}$ siRNA (Fig. 2 B). Furthermore, similar results were obtained using the $p75^{NTR}$ morpholino that selectively down-regulates $p75^{NTR}$ expression in *Xenopus* embryos (unpublished data). Therefore, pro-BDNF–induced synaptic inhibition is mediated by presynaptic but not postsynaptic $p75^{NTR}$. Expression of $p75^{NTR}$ siRNA in presynaptic neurons also attenuated the decrease in ESC amplitude by pro-BDNF (Fig. 2 C). The changes in ESC delay of onset induced by pro-BDNF were also reversed by presynaptic expression of $p75^{NTR}$ siRNA (Fig. 2 C). It was interesting to note that there was an ~40% increase in ESC amplitude at synapses in which the presynaptic neurons expressed $p75^{NTR}$ siRNA (Fig. 2 C). Based on the inhibitory effect of pro-BDNF, this may be caused by the minute, constitutive release of muscle-derived endogenous pro-BDNF, which would dampen the baseline synaptic transmission, and expression of $p75^{NTR}$ siRNA, which would remove this inhibitory effect of endogenous pro-BDNF.

Pro-BDNF–induced retraction of presynaptic terminals are also mediated by $p75^{NTR}$

To test whether pro-BDNF causes the morphological retraction of presynaptic terminals from recorded muscle cells, we labeled presynaptic neurons with GFP (green) by embryo injection. The synaptic sites were visualized by labeling postsynaptic AChRs with a low concentration of α-BTX (100 nM), which blocked only 30% of neurotransmission at these synapses (Walsh and Lichtman, 2003; unpublished data). Phototoxicity was rarely observed, and synaptic terminals did not exhibit any gross abnormality over extended fluorescence imaging sessions (>4 h). However, upon application of pro-BDNF, axon terminals actively retracted from postsynaptic sites (Fig. 3 A). Synaptic retraction was defined as withdrawal of the nerve terminal from the synaptic site by 1 µm. Within 30 min, synaptic contacts (Fig. 3 A, yellow-colored areas) were reduced dramatically. By 60 min, some withdrawing axons exhibited thick bulges that resembled retraction bulbs (Fig. 3 A). Unlike pro-BDNF–induced synaptic depression (Fig. 3 B), morphological retraction of presynaptic terminals occurred at a slower rate ($t_{1/2}$ = 35 min) than the physiological synaptic depression. Once the synaptic retraction occurred, the washout of pro-BDNF did not reverse axonal retraction (Fig. S3). It is important to note that neuronal soma remained healthy for hours after the application of pro-BDNF (Fig. 3 A, right). To further confirm that the retraction reflects an early stage of terminal withdrawal from synaptic sites, we simultaneously recorded SSCs while imaging axonal retraction. We found that pro-BDNF–induced synaptic depression occurred before terminal retraction (Fig. 4), supporting a notion that synaptic depression is a prelude that set the stage for synaptic retraction. Collectively, our physiological and morphological data suggested that cleavage-resistant pro-BDNF promotes retraction of nerve terminals from postsynaptic sites.

To further confirm that pro-BDNF–induced synaptic retraction is mediated by $p75^{NTR}$, we performed time-lapse imaging on synapses expressing $p75^{NTR}$ siRNA. The pro-BDNF–induced synaptic retraction was blocked by presynaptic expression of $p75^{NTR}$ siRNA but not by scrambled siRNA (Fig. 3 B). 1 h after pro-BDNF treatment, neurons expressing presynaptic $p75^{NTR}$ siRNA did not show axonal retraction (Fig. 3, B and C). Instead, some of the terminals exhibited elongation or expansion of axonal terminals (Fig. 3 B). Collectively, these results suggest that pro-BDNF triggers physiological depression of neuromuscular synapses and morphological retraction of presynaptic terminals via activation of $p75^{NTR}$ in the presynaptic sites.

Synaptic depression and retraction triggered by pro-BDNF from postsynaptic myocytes

To gain insight into the mechanisms by which pro-BDNF regulates synaptic retraction, we investigated whether postsynaptic muscle cells secrete pro-BDNF upon stimulation. Because of the lack of pro-BDNF–specific ELISA detection and a limited number of muscle cells in the *Xenopus* cocultures (<1,000 myocytes), biochemical measurement of activity-dependent pro-BDNF secretion from muscle cells was not feasible. Instead, we measured endogenous pro-BDNF secretion using an established cell surface–staining method based on the fact that pro-BDNF is positively charged at physiological pH and could be associated with cell surface membrane after its secretion (Nagappan et al., 2009). The muscle cell cultures were depolarized by high K^+ (50 mM) for 5 min, briefly fixed, and processed for cell surface immunofluorescence staining under membrane-impermeable conditions using a pro-BDNF–specific antibody. Western blotting of brain homogenates from wild-type and BDNF mutant mice indicated that this antibody specifically detects pro-BDNF but not mBDNF (Nagappan et al., 2009). Under the cell-impermeable conditions, antibodies against intracellular protein such as MAP2 or tau could not detect any signal in neurons in the same dish, suggesting that they did not penetrate into cells (unpublished data). At resting state, pro-BDNF was barely detectable on the muscle surface (Fig. S4 A). Upon depolarization, the cell surface pro-BDNF signal increased dramatically (88%) compared with that of unstimulated muscle cells (Fig. S4, B and C). This increase was much more pronounced when the cleavage of pro-BDNF by matrix metalloproteases (MMPs) was blocked (MMP-I; Fig. S4, B and C).

Previous studies have shown that a prolonged, repetitive depolarization of postsynaptic muscle cells (2–6 Hz and >900-3,000 pulses) induced a sustained synaptic depression (Lo and Poo, 1991; Lo et al., 1994; Cash et al., 1996). A similar approach was used to determine whether activity-induced synaptic depression is caused by the secretion of pro-BDNF from the myocytes. Whole-cell recording was switched to the current-clamp mode after a period of voltage-clamp recording, and repetitive stimulation was applied to induce action potentials in myocytes (Fig. 5 A). Changes in SSC frequency observed before and after a single episode of muscle stimulation were monitored. We found that synaptic depression depends on the number of depolarizing pulses applied to the postsynaptic

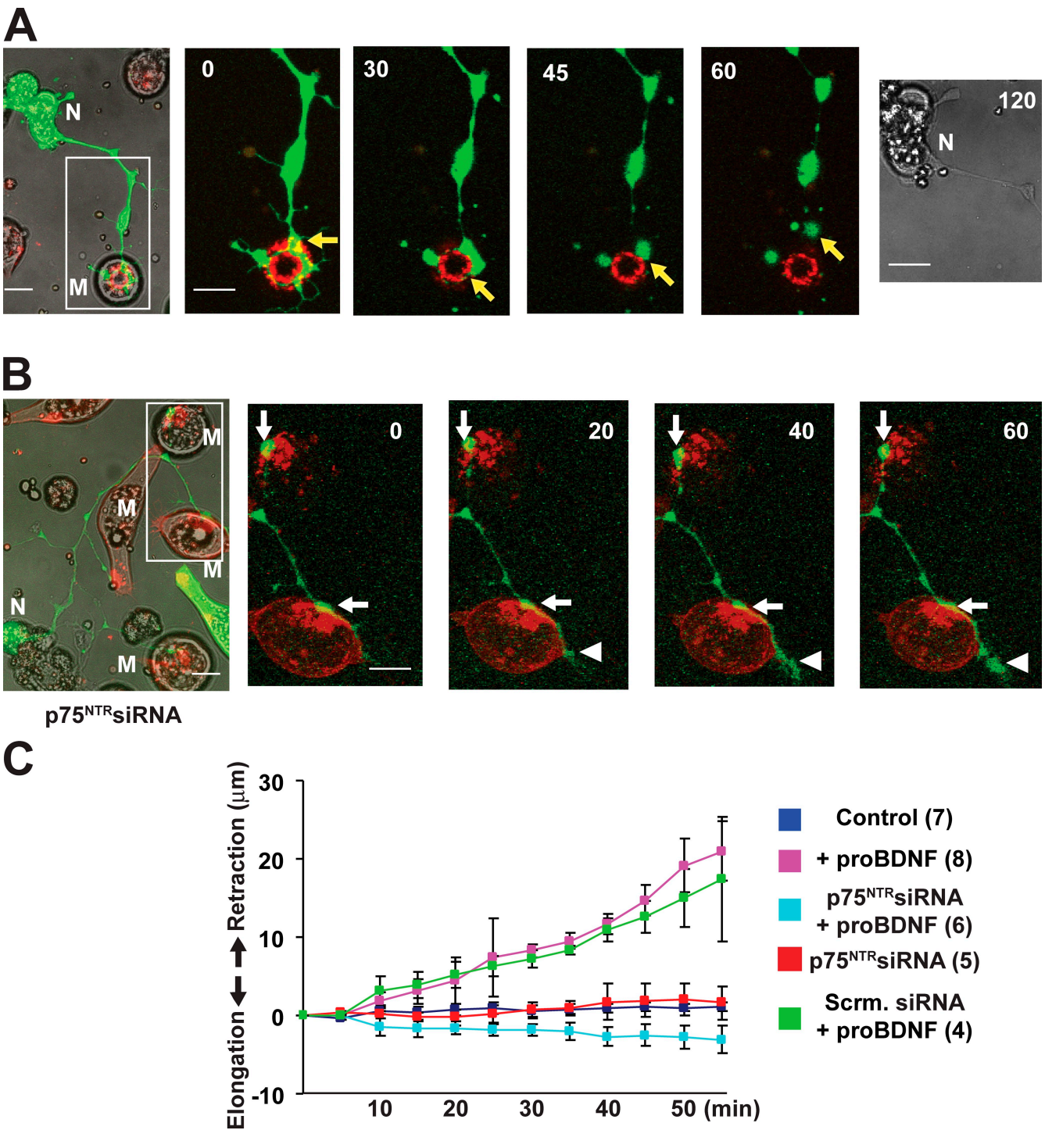

Figure 3. **Pro-BDNF–induced synaptic retraction mediated by presynaptic p75^{NTR}.** (A) Time-lapse images showing the retraction of a nerve terminal from its target myocyte (M) after pro-BDNF treatment. The spinal neuron (N) is labeled with GFP (green), and AChRs on the postsynaptic membrane are labeled with rhodamine-conjugated α-BTX (red). Pro-BDNF was applied at time 0. Enlarged images of an area within the white box are shown at the left and were captured at the indicated times (shown in minutes) after pro-BDNF application. The GFP-labeled axonal terminal (yellow arrows) clearly occupied the synaptic site (colocalized with AChRs; yellow) before treatment but progressively withdrew from the junction after pro-BDNF treatment. Note that the cell body of the neuron remained healthy even after 2 h. (B) Time-lapse images showing that pro-BDNF failed to induce retraction of an axon of a neuron expressing p75^{NTR} siRNA. Note that upon application of pro-BDNF, the terminals either did not retract (white arrows) or continued to extend further (white arrowheads). The inset is magnified to show more detailed images of the synapses. (C) Time course of synaptic retraction under different conditions. The number of experiments performed in each condition is indicated in parentheses. Error bars represent SEM. Scrm., scrambled. Bars, 10 μm.

myocytes: although a mild stimulation (1 Hz and 30 pulses) did not induce any change in synaptic efficacy, stronger stimulation (>960 pulses) reliably induced synaptic depression (Fig. S5 A).

To study the role of pro-BDNF cleavage in synaptic depression, we expressed cDNAs of cleavable (pro-BDNF–GFP) or cleavage-resistant (AA–pro-BDNF–GFP) pro-BDNF in muscle cells

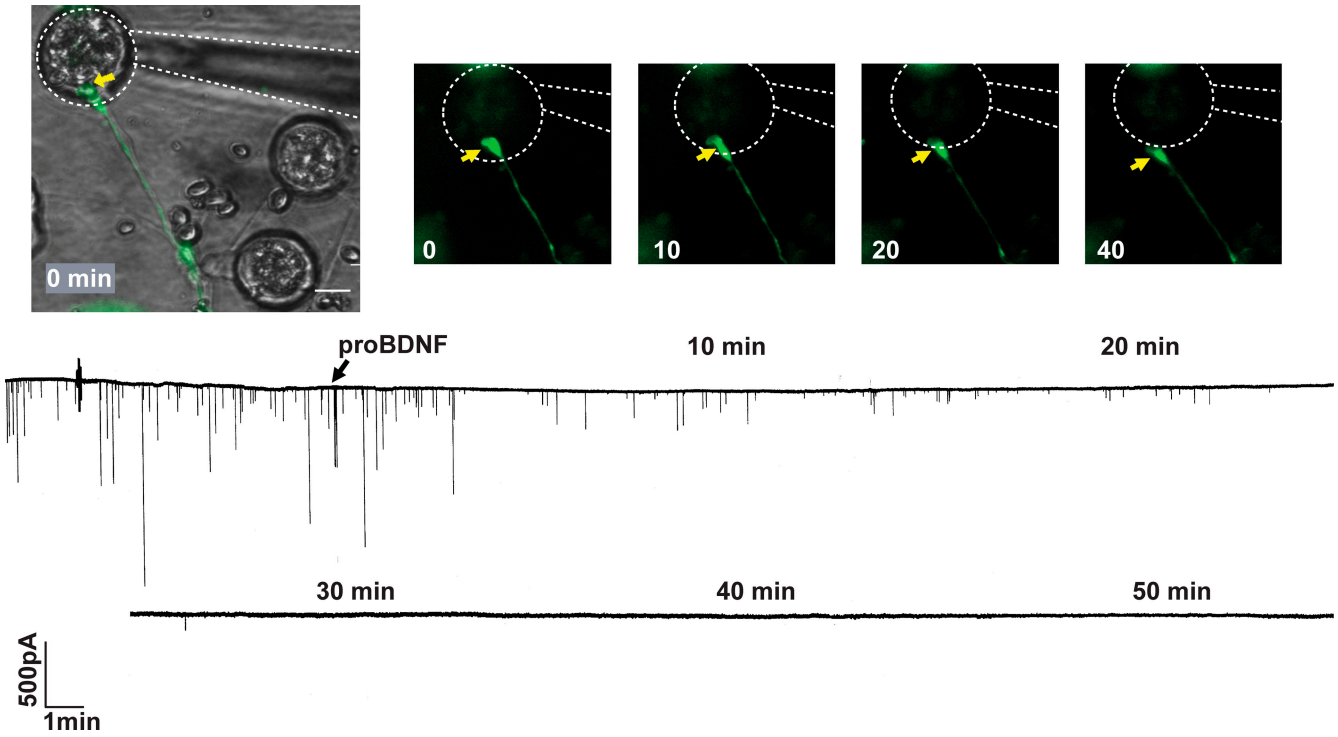

Figure 4. **Simultaneous recordings of pro-BDNF–induced synaptic depression and imaging of terminal retraction.** (top) Time-lapse images showing progressive retraction of a nerve terminal from a myocyte after pro-BDNF treatment. The dotted circle indicates the myocytes recorded; the dotted line indicates the recording pipette; the arrows indicate the axon terminal. (bottom) Simultaneous recording of SSC recording. The recording shows a rapid and persistent decrease in SSC frequency after pro-BDNF application. Note that synaptic depression precedes axonal retraction from its target myocyte. $n = 4$ independent experiments. Bar, 10 µm.

using embryo injection techniques (Yuan et al., 2003). In myocytes expressing cleavable pro-BDNF, mild stimulation (1 Hz for 30 s), which elicited no effect in control synapses, now resulted in a significant increase in SSC frequency (Fig. 5 B, left) but not amplitude (Fig. 5 D, left). The SSC frequency neither increased nor decreased after stimulation in myocytes expressing GFP only (Fig. 5 B, right).

We next expressed cleavage-resistant pro-BDNF (AA–pro-BDNF) in postsynaptic cells. Mild stimulation of myocytes (1 Hz and 30 pulses) elicited a completely opposite effect to that expressing cleavable pro-BDNF, a dramatic decrease in SSC frequency (Fig. 5 C). Further analysis of SSC amplitude indicated that postsynaptic depolarization induced a marked decrease in amplitude (Fig. 5 D, left) as well as increases in both rise and decay times of SSCs (Fig. 5 D, middle and right). These results are consistent with the notion that postsynaptic secretion of cleavage-resistant pro-BDNF elicited a retraction of presynaptic terminals. The observed reduction of SSC amplitude did not recover during the course of these experiments (Fig. 5 C), suggesting that the effect of cleavage-resistant pro-BDNF is irreversible. Thus, cleavage-resistant pro-BDNF secreted in response to postsynaptic depolarization irreversibly depressed synaptic efficacy. The dramatically opposing effects of postsynaptic stimulation suggest that activity-dependent control of pro-BDNF cleavage regulates synaptic potentiation or depression.

To further test whether strong depolarization triggers the secretion of endogenous pro-BDNF, leading to synaptic depression, we expressed $p75^{NTR}$ siRNA (together with GFP) in either pre- or postsynaptic cells. Synaptic depression was induced by strong depolarization applied to myocytes (1 Hz and 1,920 pulses). Neuronal expression of $p75^{NTR}$ siRNA but not scrambled siRNA prevented synaptic depression. As a control, expression of $p75^{NTR}$ siRNA in postsynaptic muscle cells did not prevent the depression (Fig. S5 B). These data indicated that endogenous proneurotrophins, most likely pro-BDNF (because there is little NGF and NT4 in muscle cells at this stage [Xie et al., 1997], and NT3 does not have a strong proneurotrophin-binding domain), released by muscle cell were sufficient to induce synaptic depression when strong train stimulation was applied to innervated muscle cells.

The failure of mild stimulation (1 Hz for 30 s) to induce synaptic depression in control synapses could be caused by either an insufficient amount of pro-BDNF secreted and/or a rapid conversion of some of the secreted pro-BDNF to mBDNF. To elevate pro-BDNF in the synaptic clef, we applied a cocktail of protease inhibitors before postsynaptic depolarization (Fig. 6 A), thereby preventing the conversion of pro-BDNF to mBDNF. Baseline synaptic currents were recorded for a period of 10 min followed by treatment with protease inhibitors for another 10 min while recording. The postsynaptic myocyte was then stimulated (1 Hz for 30 s), and synaptic currents were recorded for another 20–30 min. The postsynaptic stimulation now induced a marked decrease in SSC frequency (Fig. 6 B, right). This result, together with the synaptic depression trigged by a stimulation of myocytes expressing AA–pro-BDNF (Fig. 5 C), suggests an important role of proteases in pro-BDNF–induced synaptic depression. Several MMPs

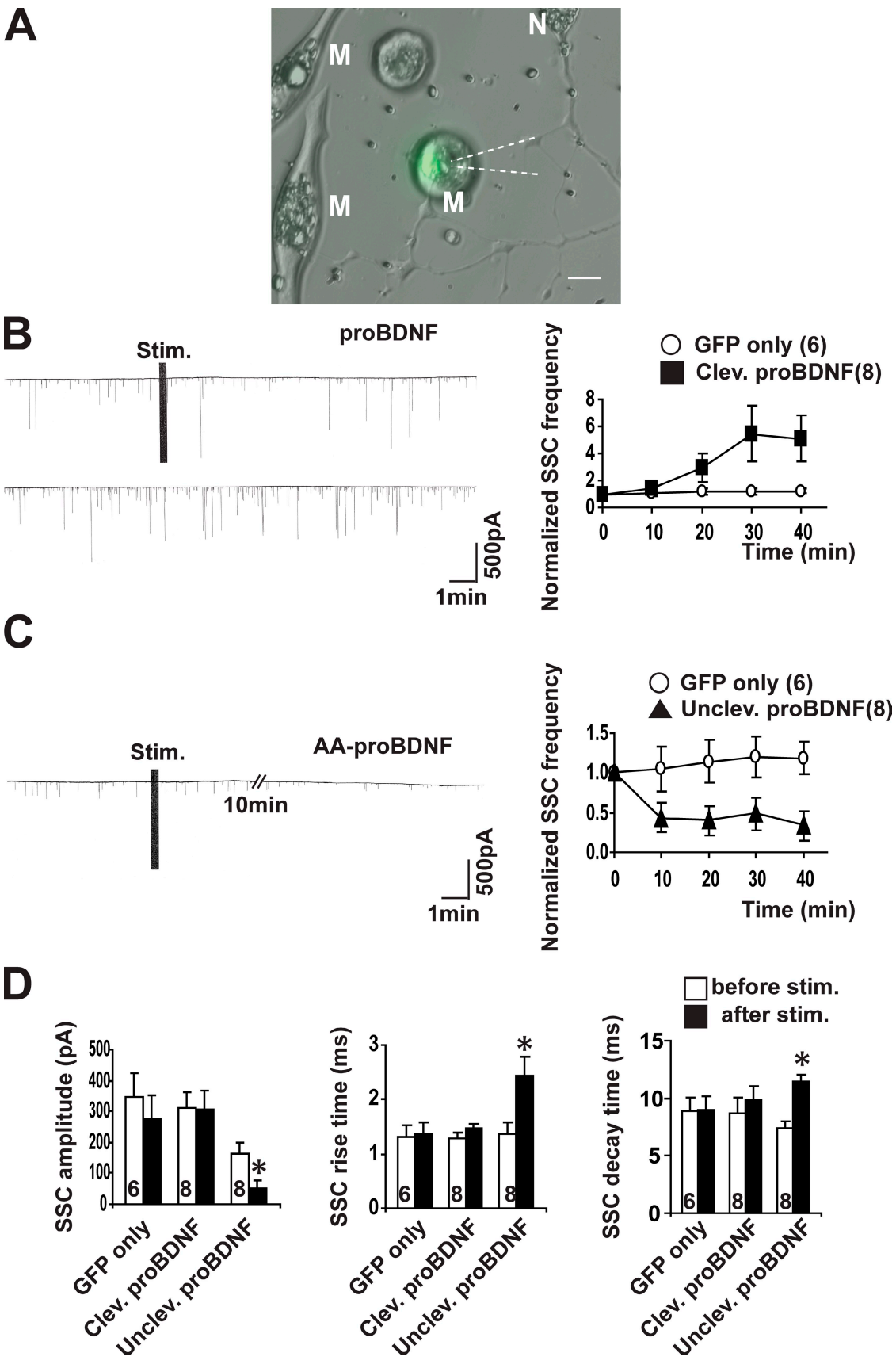

Figure 5. **Synaptic modulation elicited by stimulation of myocytes expressing cleavable and cleavage-resistant pro-BDNF.** (A) Superimposed differential interference contrast and GFP fluorescence image showing a motor neuron (N) innervating a myocyte (M) expressing cleavage-resistant pro-BDNF (green). The dashed lines indicate the recording pipette. (B and C) Examples (left) and summary (right) of SSC recordings before and after stimulation

are highly enriched at the frog and mammalian NMJs (Kherif et al., 1998; Schoser and Blottner, 1999; VanSaun and Werle, 2000). Because MMP3 and MMP9 have been shown to cleave pro-BDNF in vitro (Lee et al., 2001; Hwang et al., 2005), we further tested whether synaptic depression induced by postsynaptic stimulation in the presence of inhibitors for these MMPs could occur. Interestingly, the synaptic depression was induced when cells were treated with a combination of MMP3 and MMP9 inhibitors but not either one alone. Thus, more than one protease might be involved in the pro-BDNF to mBDNF conversion at the developing neuromuscular synapses.

Finally, to address whether pro-BDNF truly serves as a retrograde signal, we introduced a BDNF morpholino to either presynaptic motor neurons or postsynaptic myocytes by embryo injection to inhibit the expression of endogenous BDNF. BDNF morpholino but not scrambled morpholino was able to reduce the levels of endogenous BDNF protein in the whole embryos by ~40% (Fig. 7 A). Expression of BDNF morpholino in the muscle cell but not in the presynaptic neuron completely reversed synaptic depression induced by postsynaptic stimulation in the presence of metalloprotease inhibitors (Fig. 7 B). Postsynaptic stimulation in the presence of protease inhibitors also induced the retraction of presynaptic terminals (Fig. 8 A). Consistent with the physiological experiments, expression of BDNF morpholino in the postsynaptic muscle cells (Fig. 8 B) but not in the presynaptic neurons (Fig. 8 C) prevented axonal retraction. These results suggest that pro-BDNF is derived primarily from postsynaptic muscle cells. To confirm that pro-BDNF acts on presynaptic $p75^{NTR}$ to elicit its retrograde effects, we expressed $p75^{NTR}$ siRNA using embryo injection. As described in Fig. 7 A, synaptic depression was reliably induced by postsynaptic stimulation in the presence of protease inhibitors (Fig. 7 C, second bar group). The synaptic depression was selectively prevented by presynaptic (N+), but not postsynaptic (M+) expression of $p75^{NTR}$ siRNA (Fig. 7 C). Expression of scrambled siRNA had no effect on this activity-dependent synaptic depression (Fig. 7 C, last bar group). Collectively, these data suggest that, at the developing neuromuscular synapses, activity-dependent secretion of endogenous pro-BDNF from postsynaptic muscle cells triggers synaptic depression and retraction through $p75^{NTR}$ on presynaptic terminals.

Discussion

Substantial evidence suggests that one of the main functions of mBDNF in the nervous system is to strengthen synaptic connection and facilitate synaptic transmission (Poo, 2001; Lu and Je, 2003). For example, by activating TrkB, mBDNF facilitates LTP in the hippocampus and strengthens the development of ocular dominance in the visual cortex (Cabelli et al., 1995, 1997; Figurov et al., 1996). At neuromuscular synapses, acute application of mBDNF elicits a rapid increase in transmitter release (Lohof et al., 1993), whereas long-term treatment with mBDNF promotes synapse maturation (Wang et al., 1995). The discovery that pro-BDNF preferentially binds and activates $p75^{NTR}$ (Lee et al., 2001) suggests that pro-BDNF is not a biologically inactive precursor but could elicit through its own receptor physiological functions distinct from mBDNF. Although it was initially questioned whether neurons in the central nervous system (CNS) could secrete pro-BDNF (Matsumoto et al., 2008), recent studies have shown that CNS neurons primarily secrete pro-BDNF in response to depolarization when protease inhibitors were included in the experimental procedures (Nagappan et al., 2009; Yang et al., 2009). Using the neuromuscular synapse as a model system, this study has made several interesting observations. First, pro-BDNF functionally suppresses synaptic transmission and structurally causes axonal retraction. To our knowledge, this is the first demonstration of the inhibitory effects of pro-BDNF on synaptic transmission and connectivity. Second, the physiological and morphological effects pro-BDNF are mediated by $p75^{NTR}$ in the presynaptic terminals. This finding, together with the observations that pro-BDNF promotes apoptosis in sensory and sympathetic neurons (Lee et al., 2001) and facilitates hippocampal long-term depression (Woo et al., 2005), provides further support for the yin-yang hypothesis (Lu et al., 2005): proneurotrophins and mature neurotrophins elicit opposite effects through activation of $p75^{NTR}$ and Trk receptors, respectively. Third, postsynaptic stimulation, which presumably induces the secretion of BDNF from the muscle cells, could either enhance or suppress synaptic transmission, depending on whether pro-BDNF can be processed. These data provide evidence supporting the notion that BDNF is a retrograde messenger that mediates activity-dependent synaptic modulation. Finally, blockade of pro-BDNF cleavage, by either mutation of its cleavage site or inhibition of extracellular proteases, particularly the metalloproteases such as MMP3 and MMP9, facilitates synaptic depression. Thus, metalloproteases may be a major class of proteases mediating the pro-BDNF to mBDNF conversion at the *Xenopus* NMJ. These results identify pro-BDNF as a key retrograde signal that controls presynaptic development and function and suggest that proteolytic cleavage of pro-BDNF is an important mechanism controlling the direction of BDNF regulation.

Pro-BDNF as a retrograde signal for synaptic depression

Decades of research suggest that postsynaptic cells can generate positive or negative retrograde signals that affect presynaptic

of postsynaptic myocytes expressing cleavable (Clev.; B) and cleavage-resistant (uncleavable [Unclev.]; C) AA–pro-BDNF. Repetitive depolarization was applied to the postsynaptic myocytes through a whole-cell recording pipette (1 Hz for 30 s) under the current-clamp condition (Stim.). Note that at synapses expressing cleavable pro-BDNF, SSC frequency increased after postsynaptic depolarization. In contrast, at synapses expressing cleavage-resistant pro-BDNF, SSC frequency decreased after postsynaptic depolarization. The numbers in parentheses indicate the number of synapses recorded. (D) Quantitative analysis of amplitude (left), rise time (middle), and decay time (right) of SSCs before and after stimulation (Stim.) of postsynaptic myocytes expressing cleavable and cleavage-resistant pro-BDNF. The numbers in the bars indicate the number of synapses recorded. *, $P < 0.05$. (B–D) Error bars represent SEM. Bar, 10 µm.

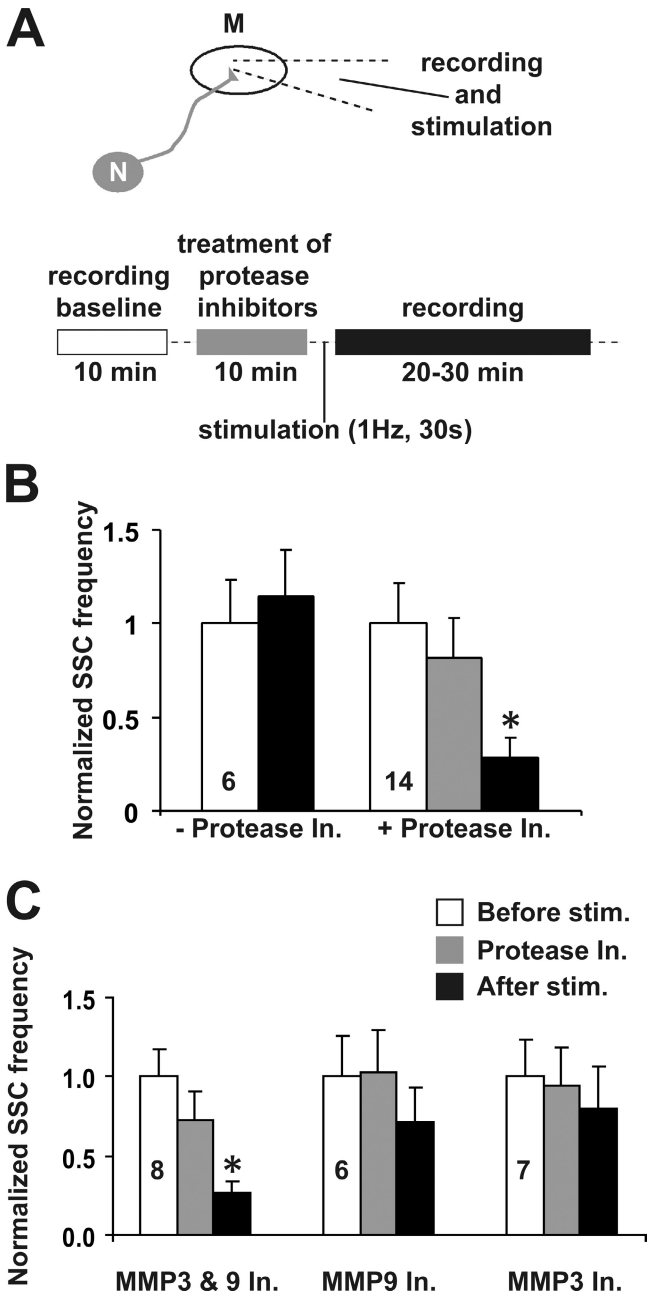

Figure 6. **Synaptic depression induced by postsynaptic secretion of endogenous pro-BDNF, which is processed by MMP3 and MMP9.** (A, top) A schematic diagram showing a synapse in which a spherical myocyte (M) is innervated by single spinal neurons (N). The dashed lines indicate the recording pipette. (bottom) The experimental protocol is shown. After baseline recording (10 min), protease inhibitors were applied for 10 min. Repetitive depolarization was applied to the postsynaptic myocytes through a whole-cell recording pipette (1 Hz for 30 s) under current-clamp condition, and synaptic efficacy was monitored. (B) Quantitative analysis of depolarization-induced depression caused by treatment with protease inhibitors (In.). Note that treatment with protease inhibitors alone or stimulation alone did not alter SSC frequency, but stimulation in the presence of protease inhibitors markedly reduced synaptic efficacy. (C) Specific MMPs involved in depolarization-induced synaptic depression. 50 nM MMP3 inhibitor, 50 µM MMP9 inhibitor, or both were applied to the cultures for at least 10 min. Synaptic depression was induced by postsynaptic stimulation (stim.) as described in Fig. 4. Note that postsynaptic stimulation in the presence of both MMP3 and MMP9 inhibitors but not either one alone triggered synaptic depression. (B and C) The numbers in the bars indicate the number of synapses recorded. Error bars represent SEM. *, $P < 0.05$.

function (Lo et al., 1994). Using *Xenopus* nerve–muscle coculture as a model, Poo and co-workers have elegantly demonstrated that postsynaptic activity is critical in functional suppression and, ultimately, the elimination of synapses, a process which is critical for proper development of neuronal circuits (Lo and Poo, 1991; Dan and Poo, 1992; Lo et al., 1994). They showed that postsynaptic depolarization elicited by repetitive stimulation of presynaptic motor neurons (Lo and Poo, 1991), repetitive acetylcholine puffing to the myocyte surface (Dan and Poo, 1992), or direct injection of depolarizing pulses into postsynaptic myocytes (Lo et al., 1994) resulted in a marked and sustained reduction in synaptic efficacy at the neuromuscular synapses. Furthermore, inhibition of postsynaptic Ca^{2+} rise by BAPTA prevents synaptic depression (Lo et al., 1994), whereas an increase in cytosolic Ca^{2+} by photo-uncaging in the postsynaptic myocytes is sufficient to induce persistent synaptic depression (Cash et al., 1996). These results suggest that postsynaptic Ca^{2+} signaling is important for the release of a factor, which in turn acts on presynaptic terminals to induce synaptic depression. The nature of the retrograde factor remains unknown.

In this study, we provide evidence that one such factor is pro-BDNF. Application of exogenous pro-BDNF elicited rapid synaptic depression, and such depression was sustained as long as pro-BDNF was present. Pro-BDNF also induced the retraction of presynaptic terminals, albeit in a slower time scale. Stimulation of postsynaptic cells expressing cleavage-resistant pro-BDNF also induced a sustained depression. A much milder postsynaptic depolarization (1 Hz for 30 s) compared with the one used previously (Lo et al., 1994; 6 Hz for 20 min) was sufficient to induce depression under our experimental conditions, perhaps because of an elevated level of pro-BDNF by overexpression or protease inhibitors that prevent endogenous pro-BDNF conversion. Our experiments suggest that the postsynaptically derived pro-BDNF acts on presynaptic $p75^{NTR}$ to induce synaptic depression. It appears that pro-BDNF is only expressed in postsynaptic myocytes, whereas $p75^{NTR}$ is only expressed in presynaptic motor terminals at the *Xenopus* neuromuscular synapses (Fig. S1, B and C). Moreover, both morphological and physiological effects were completely blocked by inhibiting presynaptic but not postsynaptic $p75^{NTR}$. It should be noted that these effects are not the consequences of motor neuron apoptosis because there was no apparent change in cell viability 24 h after pro-BDNF exposure (Fig. S1 E) and pro-BDNF–induced synaptic depression can be completely reversed upon removal of pro-BDNF within 5–10 min (Fig. 1 B). We acknowledge that there has been no direct evidence so far that endogenous pro-BDNF is the key factor for synaptic depression in vivo. Finally, several recent studies have now confirmed that pro-BDNF is the major form secreted from CNS neurons (Nagappan et al., 2009; Yang et al., 2009). Although it is practically impossible to demonstrate pro-BDNF secretion at the synaptic cleft, cell surface staining with a pro-BDNF–specific antibody showed that depolarization induces the secretion of pro-BDNF from myocytes (Fig. S4). Collectively, our data support a model showing that postsynaptic depolarization triggers the secretion of pro-BDNF, which in turn acts on presynaptic $p75^{NTR}$ to induce synaptic depression and axon retraction.

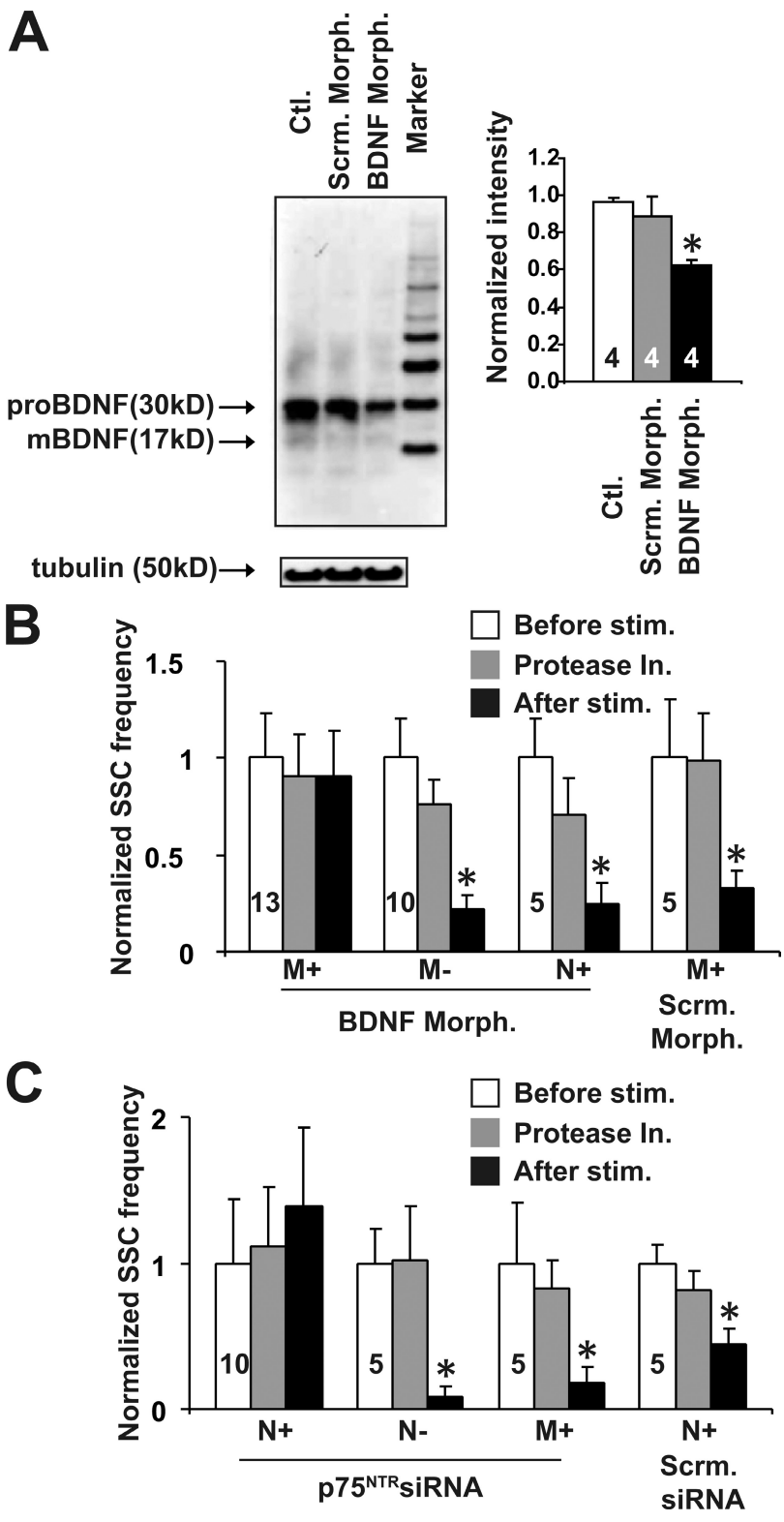

Figure 7. **Synaptic depression induced by postsynaptic secretion of endogenous pro-BDNF, which activates presynaptic p75^{NTR}.** (A) Down-regulation of pro-BDNF by BDNF morpholino. *Xenopus* BDNF–specific morpholino (Morph.) and scrambled (Scrm.) analogues were introduced by embryo injection. Neural tubes were dissected, and proteins were extracted. Western blots were performed using anti-BDNF antibodies. The blot was reprobed with an antitubulin antibody for loading controls. Note a reduction of pro-BDNF expression in BDNF morpholino–injected but not in uninjected (control [Ctl.]) or scrambled morpholino–injected embryos (left). Quantitative analysis of pro-BDNF expression in four independent experiments (right) is shown. The numbers in the bars indicate the number of Western blots performed. (B) Effect of presynaptic (N+) or postsynaptic (M+) expression of BDNF morpholino on depolarization-induced depression. (C) Effect of presynaptic or postsynaptic expression of p75^{NTR} siRNA on depolarization-induced depression. (B and C) The numbers in the bars indicate the number of synapses recorded. (A–C) Error bars represent SEM. *, $P < 0.05$. In., inhibitor; stim., stimulation.

Proteolytic conversion of pro-BDNF to mBDNF at the NMJ

A brief, repetitive presynaptic stimulation has been shown to induce a rapid and sustained increase in synaptic efficacy at the *Xenopus* neuromuscular synapses (Wan and Poo, 1999). Curiously, a much higher frequency (40–60 Hz) should be applied to induce such a strong synaptic potentiation. We have recently found that in hippocampal neurons, high frequency (such as theta burst) but not low frequency (1 Hz) stimulation preferentially induces the secretion of proteases, which in turn converts pro-BDNF to mBDNF extracellularly in hippocampal neurons (Nagappan et al., 2009). Extracellular conversion of pro-BDNF to mBDNF has been shown to be critical for hippocampal late-phase LTP (Pang et al., 2004). Thus, it is possible

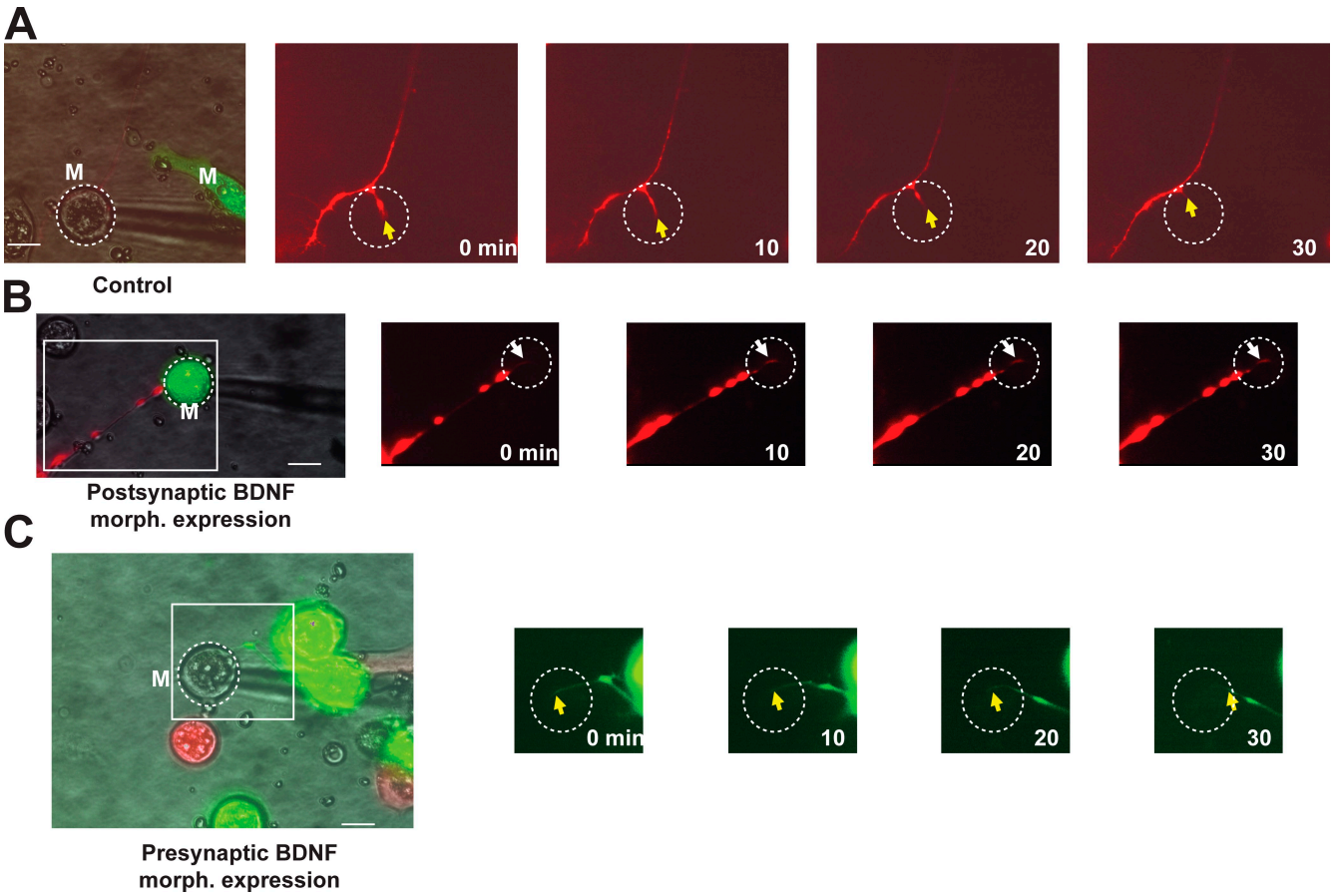

Figure 8. **Synaptic retraction induced by postsynaptic secretion of endogenous pro-BDNF.** Nerve terminals were labeled by rhodamine-dextran (red). The expression of BDNF morpholino (morph.) is indicated by the green fluorescence. Repetitive depolarization was applied to the postsynaptic myocytes (M) through a whole-cell recording pipette (2 Hz for 2 min) under current-clamp condition, and the axon terminal was visualized by time-lapse microscopy. (A) Synaptic retraction induced by repetitive postsynaptic stimulation. The axon was filled with rhodamine-dextran to visualize the axon terminal. After 30 min, the axon terminal from a stimulated myocyte retracted (indicated by yellow arrows). (B and C) Effect of presynaptic (B) or postsynaptic (C) expression of BDNF morpholino on depolarization-induced synaptic retraction. Postsynaptic expression of BDNF morpholino in myocytes blocked synaptic retracted induced by repetitive postsynaptic stimulation (indicated by white arrows). However, presynaptic expression of BDNF morpholino in spinal neurons could not block the depolarization-induced synaptic retraction (indicated by yellow arrows). The insets are magnified to show more detailed images of the synapses. (A–C) The dotted circles indicate myocytes recorded with a patch electrode. Bars, 10 µm.

that postsynaptically derived pro-BDNF could be converted to mBDNF by proteases secreted from presynaptic terminals, leading to synaptic potentiation. Several lines of evidence support this hypothesis. First, we found that postsynaptic stimulation with our protocol (1 Hz for 30 s) was not sufficient to unmask pro-BDNF–mediated synaptic depression. However, treatment with protease inhibitors before postsynaptic depolarization induced a robust synaptic depression (Fig. 6 B). Moreover, stimulation of myocytes expressing cleavable pro-BDNF resulted in synaptic potentiation rather than depression (Fig. 5 B). Second, MMPs are expressed in motor neurons and are highly enriched at the NMJ (Kherif et al., 1998; Schoser and Blottner, 1999; VanSaun and Werle, 2000). Our electrophysiology experiments showed that more specific inhibitors for metalloproteases MMP3 and MMP9 together could unmask the depolarization-induced synaptic depression (Fig. 7 C), suggesting that MMP3 and MMP9 may be the proteases that convert pro-BDNF into mBDNF upon synaptic activity. Postsynaptic depolarization also induced axonal retraction in the presence of protease inhibitors (Fig. 8 A). Third, using a fluorescence resonance energy transfer–based fluorescence beacon assay, we showed that stimulation of motor neurons induced the cleavage of a peptide containing the cleavage sequence in pro-BDNF, and such cleavage is likely to be mediated by neuronal secretion and/or activation of MMP3 and MMP9 (unpublished data). Finally, our cell surface–staining experiments using antibodies specific for pro-BDNF or mBDNF showed that the majority of the secreted BDNF is the pro form, and cell surface staining of secreted pro-BDNF was dramatically increased when depolarization of myocytes was coupled with treatments of MMP inhibitors (Fig. S4). We further showed that stimulation of presynaptic neurons with glutamate induces an increase in mBDNF staining in the surface of myocytes, and such staining was decreased when neurons were stimulated in the presence of MMP inhibitors (unpublished data). Future studies should be directed toward demonstrating that high frequency stimulation induces activation of MMP3 and MMP9 at the neuromuscular synapses and that conversion of pro-BDNF to mBDNF is responsible for activity-dependent synaptic potentiation at NMJs and other synapses in vivo.

Materials and methods

DNA constructs, embryo injection, and *Xenopus* nerve–muscle coculture
EGFP–pro-BDNF and AA–pro-BDNF–GFP cDNA constructs were made as previously described (Egan et al., 2003). *Xenopus* egg laying was induced by injecting female *Xenopus* with human chorionic gonadotropin hormone (Sigma-Aldrich). Resulting eggs were fertilized with sperm derived from male testis. Morpholinos, siRNA, or cDNAs were mixed with fluorescence dye (FITC or rhodamine) or 1 µg/ml GFP mRNA in a 1:1 ratio and injected into one of the blastomeres at the 2–4- or 8–16-cell stage using the Picospritzer pressure ejector (Parker Hannifin). As such, neurons and muscle cells derived from the injected blastomere, which were identified by their exhibition of fluorescence, underwent changes in the expression of genes of interest. 1 d after injection, the neural tube and associated myotomal tissues were dissected, dissociated in Ca^{2+}-Mg^{2+}–free medium (58.2 mM NaCl, 0.7 mM KCl, and 0.3 mM EDTA, pH 7.4) for 15–20 min, and plated on glass coverslips. Cells were grown for 1 d in culture medium consisting (vol/vol) of 50% L-15 medium, 1% fetal calf serum, and 49% Ringer's solution (117.6 mM NaCl, 2 mM $CaCl_2$, 2.5 mM KCl, and 10 mM Hepes, pH 7.6). After 1 d in vitro, spinal neurons and myocytes form synapses ad lib. The mixing of cells derived from injected and uninjected blastomeres resulted in the formation of synapses with altered expression of genes of interest in presynaptic neurons and/or postsynaptic muscle cells, as indicated by fluorescence.

Morpholino and siRNA
Position 45–67 relative to the start codon of the open reading frame, which is shared between the two *Xenopus* $p75^{NTR}$ genes (*p75NTRa* and *p75NTRb*; Hutson and Bothwell, 2001), was selected (5′-AGAGCCAUGUUGGUCAGGGCA-3′) to generate $p75^{NTR}$ siRNA. The 23-nt sense and 23-nt antisense strands with two base overhangs (AA) were chemically synthesized by Thermo Fisher Scientific in deprotected and desalted form. Scrambled $p75^{NTR}$ siRNA (5′-GCUGGCCGAGGCUUAAGAGAU-3′) was used as a control. Antisense morpholino oligonucleotides, which achieve their effects by inhibiting translation initiation through its binding to the 5′ untranslated region of the target mRNA, were used to down-regulate the expression of *Xenopus* genes. The *Xenopus* $p75^{NTR}$ morpholino sequence was 5′-CCATGCTGATCCTAGAAAGCTGATG-3′. Its scrambled control was 5′-CTACTGCAAACATGGTACTGCTAGG-3′ (invert antisense). Anti–*Xenopus* BDNF morpholino (5′-CTCACCTGATGGAACTTATTTTAGC-3′), which is specific to *Xenopus* BDNF, and the control morpholino oligonucleotides with a scrambled sequence (5′-CCTCTTACCTCAGTTACAATGTATA-3′) were synthesized by Gene Tools, LLC. To visualize their distributions, all morpholino oligonucleotides were tagged with a fluorophore (FITC). The effectiveness of $p75^{NTR}$ siRNA and BDNF morpholino was confirmed by Western blotting (Fig. 2). All of the electrophysiological and imaging experiments on synaptic depression and retraction were performed in blind manners such that the experimenter did not know whether the fluorescent cells expressed siRNAs/morpholinos for scrambled or target genes.

Electrophysiology
Synaptic currents were recorded from innervated muscle cells in 1-d-old cultures by whole-cell recording in culture medium at room temperature (Wang et al., 1995). Neuron/myocyte pairs were selected randomly. For recordings of cells with gene manipulations, we performed blind recordings followed by fluorescence microscopy to verify whether the mRNA, cDNA, or siRNA of interest was expressed in the presynaptic motoneuron, postsynaptic muscle cell, or both. The internal pipette solution contained 150 mM KCl, 1 mM NaCl, 1 mM $MgCl_2$, and 10 mM Hepes buffer, pH 7.2. The membrane potentials of the muscle cells recorded were generally in the range of −55 to −75 mV and were voltage clamped at −70 mV. To elicit ESCs, square current pulses (0.5–1 ms and 0.5–5 V) were applied to the soma of spinal neurons with a patch electrode filled with Ringer's solution at the neuronal soma under loose seal conditions. To depolarize muscle cells, square pulses (pulse duration, 0.5 ms; amplitude, 0.8 nA) at a low rate (1 Hz and 30 pulses) were applied to the myocytes using the recording patch pipette. This stimulation protocol did not elicit synaptic depression when only GFP is expressed postsynaptically. In contrast, a stronger protocol (1 Hz and 1,920 pulses) similar to the one that Lo et al. (1994) used (2–6 Hz and >900–3,000 pulses) induced a pronounced synaptic depression in GFP-expressing myocytes (Fig. S4). Thus, the number of pulses correlates with the degree of synaptic depression.

All data were collected by a patch clamp amplifier (Axopatch 200B; MDS Analytical Technologies), with a current signal filter set at 3 kHz. Pipette and membrane capacitance and serial resistance were compensated. In all experimental conditions, the background noise was <5 pA. A threshold was set to 30 pA for SSCs because very few SSC amplitudes were <30 pA at the *Xenopus* NMJ. SSC frequency is defined as the number of SSC events per minute. The amplitude, rise time, decay time, and delay of onset of synaptic currents were analyzed using Clampfit software (MDS Analytical Technologies).

Western blot analysis
Xenopus embryos at stage 22 were quickly homogenized in extraction buffer I of the ProteoExtract Native Membrane Protein Extraction kit (EMD) according to manufacturer's instructions in the presence of protease inhibitor cocktail (set III; EMD). After high speed centrifugation (14,000 *g*), the supernatants were transferred to a fresh tube containing 300 µl Freon (1,1,2-trichlorotrifluoroethane; Sigma-Aldrich), vortexed for 1 min, incubated on ice for 5 min, and centrifuged again to remove yolk protein. To measure pro-BDNF expression, immunoprecipitation was performed. The supernatants (cytoplasmic fraction) were measured for protein concentration, and an equal amount of protein was then precleared and immunoprecipitated by chicken anti–human BDNF (2 µg for 500 µg of total protein; Lee et al., 2001) and chicken IgY agarose (Millipore). The precipitated materials were subjected to Western blotting using polyclonal anti-BDNF (1:1,500; N-20; Santa Cruz Biotechnology, Inc.). For membrane proteins ($p75^{NTR}$ and TrkB), the insoluble pellets after cytoplasmic extraction were solubilized in modified radioimmunoprecipitation assay buffer containing 1% SDS. After centrifugation at 14,000 *g* to remove insoluble material, the supernatant was measured for protein concentration, and 30 µg of protein was separated on SDS–polyacrylamide electrophoresis, and blotted onto Immobilon-P membrane (Millipore). The blots were probed with the following primary antibodies: polyclonal antibody against mouse intracellular domain of $p75^{NTR}$ (1:3,000; provided by B. Carter and P. Barker [Vanderbilt University Medical Center, Nashville, TN], M. Bothwell [University of Washington, Seattle, WA], and M. Chao [New York University, New York, NY]), chicken polyclonal anti–human TrkB (1:1,000; provided by L. Reichardt [University of California, San Francisco, San Francisco, CA] and M. Chao), and polyclonal rabbit antitubulin (1:5,000; Abcam). After thorough washes, the blots were reacted with a secondary antibody conjugated with HRP. Signals were detected by the ECL Plus kit (GE Healthcare), exposed on HyperFilm (GE Healthcare) for band intensities in linear range, scanned, and quantified using ImageJ version 1.37 (National Institutes of Health).

To determine the expression of pro-BDNF in muscle cells, 10–50 mg of muscle tissues from the hindlimbs of neonatal mice or *Xenopus* were homogenized in modified radioimmunoprecipitation assay buffer with protease inhibitor cocktail and sonicated, and proteins were extracted for 15 min by increasing SDS and Triton X-100 to 1% and were subsequently centrifuged to remove insoluble materials. The supernatant was estimated for protein concentration, and 30 µg of protein was separated on 4–12% Bis-Tris NuPAGE, transferred to Immobilon-P membrane, blocked using 5% BSA in TBST (TBS with Tween 20), probed overnight with chicken polyclonal pro-BDNF antibody (Millipore) in 3% BSA/TBST, washed, and developed using anti–chicken secondary antibody conjugated to HRP (IgY-HRP; 1:5,000; Promega) and the ECL Plus kit.

Time-lapse microscopy
Confocal imaging was performed using an inverted laser-scanning microscope (LSM 510 META; Carl Zeiss, Inc.) with a 25× NA 1.0 or 40× NA 1.3 oil immersion objective (Plan-Apochromat; Carl Zeiss, Inc.). For dual or triple color imaging, excitation lines of an argon laser of 488 nm and two helium lasers of 543 nm and 640 nm were used. Fluorescence was detected using a 458/514-nm dichroic beam splitter and a 530–560-nm band-pass filter for FITC, a 580–620-nm band-pass filter for rhodamine, and a 650-nm long-pass filter for Cy5. With the narrow band-pass filters, any crossover or bleed-through of fluorescence was eliminated. Time-lapse scanning was performed using LSM 510 imaging system software (Carl Zeiss, Inc.). After acquisition, images were processed with the LSM 5 Image Browser (Carl Zeiss, Inc.) and Photoshop CS software (Adobe). One phase-contrast image and subsequent fluorescent images were recorded every 5 or 10 min with z-series stack at 1.0-µm intervals. The expression of fluorescent dyes or siRNA did not affect axon morphology compared with uninjected controls. Axons were reconstructed three-dimensionally. For time-lapse confocal imaging, identical settings (acquisition speed, pinhole size, laser intensities, dichroics, filters, size of uncaging region of interest (ROI), uncaging iterations, etc.) were used except for the gain because of the heterogeneity of fluorescence signals. We also tested the photo-bleaching effects. Even after 6 h, the level of photo-bleaching was <10% of the fluorescence signal. Furthermore, to circumvent focal point changes during long-term imaging, several z stacks (7–10 stacks) were acquired and later

projected to two dimensions with maximum intensity. After image acquisition, threshold was adjusted for better visualization. Finally, we used high powered differential interference contrast optics to trace the remnant of the axon terminals to ensure the entire axon arbor was efficiently visualized.

Quantification of axon elongation and retraction

Using the ROI tool from the IPLab software (BD), the optical center of mass (COM) of a given axon terminal was identified. For single muscle-innervating axons, the distances between the COM of the AChR fluorescence signal and the COM of the axon terminal were determined at different time points after pro-BDNF application. The extent of retraction (or elongation) was calculated by subtracting the distance at a given time point after neuronal stimulation with that before stimulation. The values for multiple axons in the same condition were pooled and averaged. Synaptic retraction was defined as withdrawal of nerve terminal from synaptic site by 1 µm.

Immunofluorescence staining of *Xenopus* cultures

Xenopus neurons and muscle cells grown on coverslips were washed with PBS, fixed with 4% paraformaldehyde in PBS for 30 min at room temperature, incubated in 0.1% $NaBH_4$ (sodium borohydrate) in PBS to reduce autofluorescence, and blocked using 5% nonfat milk in PBS for 60 min. For pro-BDNF surface staining, the cultures were incubated with pro-BDNF antibody (1:200; Millipore) in 5% nonfat milk overnight at 4°C. The cultures were then reacted with secondary antibody (Alexa Fluor antibodies from Invitrogen) for 1 h. After PBS washes, the coverslips were rinsed with water and then mounted on medium containing Mowiol 4-88 and the antifade DABCO (1,4-diazabicyclo[2.2.2]octane). Images were acquired using a 63× NA 1.4 oil Plan-Apochromat lens and multitrack option in the LSM 510 Meta for all samples on the same day under identical conditions (laser power, pinhole, gain, and offset for two different colors). For quantitative analysis of pro-BDNF fluorescence signals, we first subtracted background and adjusted the threshold to 50% over the background fluorescence intensity by averaging the numbers obtained from three nonfluorescent areas. The dynamic range of fluorescence intensity values was confined to arbitral fluorescence unit in 8 bits (in pixels, 0 [minimum]–255 [maximum]) to normalize fluorescent signals from differently treated groups. Mean intensities from all positively stained spots along the synaptic area in a myocyte were obtained using the ROI tool in IPLab software. Then, the mean intensity values of fluorescence signal in a given synapse were averaged and presented as mean ± SEM.

For immunofluorescence staining of TrkB, $p75^{NTR}$, and intracellular pro-BDNF, similar procedures were used except that cells were permeabilized with 0.05% Triton X-100 in PBS for 5 min. After blocking, cells were incubated with TrkB antibody (1:50; Santa Cruz Biotechnology, Inc.) or $p75^{NTR}$ intracellular domain antibody (1:100; provided by B. Carter) overnight at 4°C.

Purification of recombinant pro-BDNF

To generate pro-BDNF with impaired proteolytic cleavage, residues RR were mutated to AA using PCR, and six His residues were added at the C terminus. This cDNA construct was subcloned to the expression vector pcDNA, and stably transfected HEK293 cells were isolated after selection in G418-containing medium. Cells were incubated in serum-depleted media for 18 h, and the media were collected and depleted of cells by centrifugation. His-tagged cleavage-resistant pro-BDNF was purified by Ni-bead chromatography (Xpress System Protein Purification; Invitrogen) according to the manufacturer's instructions at 4°C overnight and eluted with the use of 350 mM imidazole. Fractions containing purified His-tagged cleavage-resistant pro-BDNF were dialyzed against *Xenopus* Ringer solution (117.6 mM NaCl, 2 mM $CaCl_2$, 2.5 mM KCl, and 10 mM Hepes, pH 7.6). Proteinase inhibitors (final concentrations: 25 mM GM6001, 100 nM α_2-antiplasmin, and 10 µM ε-amino-*n*-caproic acid) were added to the dialyzed protein, and purified proteins were stored at −80°C before use. Purification was monitored by Western blotting using antibody against mBDNF and silver staining using mBDNF as a standard.

To generate a large quantity of pro-BDNF for in vivo injection experiments, we generated a stable clone of HEK293 cells using the lentiviral vector pLV1 expressing HA–pro-BDNF from a cytomegalovirus promoter. The HEK-LV/HA–pro-BDNF cells were lysed in buffer containing 50 mM Tris-HCl, pH 7.5, 150 mM NaCl, 0.1% NP-40, and protease inhibitors, sonicated, and centrifuged to remove any insoluble material. HA-tagged pro-BDNF was purified on the anti-HA affinity matrix (Roche). Protein purity was verified by silver staining (a single band), and its identity was confirmed by Western blot analysis using polyclonal anti–pro-BDNF antibody (1:1,500; N-20; Santa Cruz Biotechnology, Inc.). The concentration of pro-BDNF was determined by Bio-Rad Laboratories protein assay, and 2 ng/ml of pro-BDNF was used in all of our experiments. The relative potency of pro-BDNF purified from cell lysate, measured by its efficacy on synaptic depression at *Xenopus* neuromuscular synapses as in Fig. 1 A, was 5–10 times less than pro-BDNF secreted in the aforementioned medium of HEK293 cell culture.

Simultaneous imaging and recording of synaptic retraction

Synaptic currents were recorded from innervated muscle cells in 2-d-old *Xenopus* nerve–muscle cocultures by whole-cell recording as described in DNA constructs, embryo injection, and *Xenopus* nerve–muscle coculture. Repetitive postsynaptic stimulation in the presence of protease inhibitors was used to induce synaptic depression (Fig. 6) and terminal retraction (Fig. 8). Muscle cells were depolarized (V_H from −60 mV to −20 mV for 300 ms) at 2 Hz for a period of 6 min by injection of whole-cell currents into the myocyte under the voltage-clamp condition through the whole cell–recording pipette. During the entire course of electrophysiological recording, neurons labeled with FITC-dextran were illuminated with brief pulses of 488-nm excitation light, and fluorescence images (505 nm to 550 nm) were collected on an inverted microscope (TE1000; Nikon) with a 40× NA 0.60 air objective (Plan-Apochromat; Nikon) and a charge-coupled device (Cascade 512B; Roper Scientific). Brief UV exposure (250 ms) did not affect the baseline recording. Fluorescence and bright-field images were acquired every 10 min as long as the whole-cell recording was maintained and subsequently were processed with IPLab software offline.

Cell survival assay

Cell survival was assessed by using TUNEL labeling (In situ Cell Death Detection kit, Fluorescein; Roche). Cultures were fixed in 4% formaldehyde in PBS, permeabilized with 0.1% Triton X-100 and blocked with 5% BSA in PBS. TUNEL reaction mixture was then added to cultures for 1 h. After counting the number of TUNEL-positive and -negative neurons, cell survival was defined by the percentage of TUNEL-negative cells compared with total cell numbers.

FM 1-43 imaging

For FM dye imaging, the fluorescent styryl membrane dye FM 1-43 (Invitrogen) was loaded into *Xenopus* spinal neurons by applying high K^+ loading solution (60 mM KCl, 57.6 mM NaCl, 3.5 mM $CaCl_2$, and 10 mM Hepes, pH 7.6; 2 µM FM 1-43) to control or pro-BDNF–treated cultures for 2 min. Cells were rinsed extensively with Ringer's solution to remove membrane-bound FM dye. Next, fluorescent images of FM dye were acquired by a cool charge-coupled device camera (MicroMax 1300; Roper Scientific), mounted on an inverted epifluorescence microscope (IX70; Olympus), and analyzed offline using IPLab software. Fluorescence images were taken with a 1,000-ms exposure time with a 40× NA 0.55 objective (Plan-Apochromat; Olympus). The pseudocolor (green) was assigned to fluorescent images. FM dye destaining experiments were performed as described previously (Ryan et al., 1993; Je et al., 2005) with minor modifications. In brief, FM 1-43 was loaded into neurons as described above for 2 min, and cells were washed extensively with Ringer's solution. Fluorescence images were acquired at a rate of 0.2 Hz with a 250-ms exposure time with a 40× NA 0.6 objective. After acquiring five images (10 s) as a baseline, FM 1-43 destaining was initiated by rapid perfusion of high K^+ loading solution (60 mM KCl, 57.6 mM NaCl, 2.0 mM $CaCl_2$, and 10 mM Hepes, pH 7.6). The image data were stored and analyzed offline by IPLab software. Fluorescence intensities were extracted from time-lapse images of individual boutons. The data were normalized to background fluorescence and fitted by single exponential curves, and time constants (τ) were obtained and averaged in Excel (Microsoft).

Online supplemental material

Fig. S1 shows expression of pro-BDNF, $p75^{NTR}$, and TrkB in *Xenopus* nerve–muscle coculture system and in vivo and survival of spinal neurons upon pro-BDNF treatment using TUNEL assay. Fig. S2 shows the effect of pro-BDNF on FM 1-43 destaining kinetics. Fig. S3 demonstrates persistent synaptic retraction after pro-BDNF washout. Fig. S4 shows pro-BDNF surface staining on *Xenopus* nerve–muscle cocultures. Fig. S5 indicates synaptic depression triggered by different postsynaptic depolarization protocols and shows that $p75^{NTR}$ knockdown in spinal neurons blocked synaptic depression induced by stronger postsynaptic stimulation (1 Hz and 1,920 pulses). Online supplemental material is available at http://www.jcb.org/cgi/content/full/jcb.200811147/DC1.

We thank Drs. Phillip Nelson, Neil Shneider, Keri Martinowitch, Jay Chang, Angela Mabb, Thomas Newpher, and Newton Woo for their thoughtful comments and suggestions, and Regeneron Pharmaceuticals for providing

recombinant BDNF. We also thank Henry Teng and Saundrene Wright for assistance in preparing pro-BDNF. We express our gratitude to Drs. Bruce Carter, Mark Bothwell, Moses Chao, and Phil Barker for antibodies to p75 and Louis Reichardt and Moses Chao for antibodies to TrkB. Microscopy imaging was performed at the Porter Neuroscience Center Light Imaging Facility with the assistance of Dr. Carolyn Smith (National Institutes of Health, Bethesda, MD).

The study was supported by the National Institute of Mental Health and National Institute of Child Health and Human Development intramural research programs to B. Lu and National Institutes of Health grants to B. Hempstead.

Submitted: 26 November 2008
Accepted: 20 April 2009

References

Balice-Gordon, R.J., C.K. Chua, C.C. Nelson, and J.W. Lichtman. 1993. Gradual loss of synaptic cartels precedes axon withdrawal at developing neuromuscular junctions. *Neuron*. 11:801–815.

Cabelli, R.J., A. Horn, and C.J. Shatz. 1995. Inhibition of ocular dominance column formation by infusion of NT-4/5 or BDNF. *Science*. 267:1662–1666.

Cabelli, R.J., D.L. Shelton, R.A. Segal, and C.J. Shatz. 1997. Blockade of endogenous ligands of trkB inhibits formation of ocular dominance columns. *Neuron*. 19:63–76.

Cash, S., Y. Dan, M.M. Poo, and R. Zucker. 1996. Postsynaptic elevation of calcium induces persistent depression of developing neuromuscular synapses. *Neuron*. 16:745–754.

Chao, M.V., and M. Bothwell. 2002. Neurotrophins: to cleave or not to cleave. *Neuron*. 33:9–12.

Constantine-Paton, M., H.T. Cline, and E. Debski. 1990. Patterned activity, synaptic convergence, and the NMDA receptor in developing visual pathways. *Annu. Rev. Neurosci.* 13:129–154.

Dan, Y., and M.M. Poo. 1992. Hebbian depression of isolated neuromuscular synapses in vitro. *Science*. 256:1570–1573.

Dan, Y., Y. Lo, and M.M. Poo. 1995. Plasticity of developing neuromuscular synapses. *Prog. Brain Res.* 105:211–215.

Debski, E.A., and H.T. Cline. 2002. Activity-dependent mapping in the retinotectal projection. *Curr. Opin. Neurobiol.* 12:93–99.

Egan, M.F., M. Kojima, J.H. Callicott, T.E. Goldberg, B.S. Kolachana, A. Bertolino, E. Zaistev, B. Gold, D. Goldman, M. Dean, et al. 2003. The BDNF val66met polymorphism affects activity-dependent secretion of BDNF and human memory and hippocampal function. *Cell*. 112:257–269.

Figurov, A., L.D. Pozzo-Miller, P. Olafsson, T. Wang, and B. Lu. 1996. Regulation of synaptic responses to high-frequency stimulation and LTP by neurotrophins in the hippocampus. *Nature*. 381:706–709.

Goda, Y., and G.W. Davis. 2003. Mechanisms of synapse assembly and disassembly. *Neuron*. 40:243–264.

Hensch, T.K. 2005. Critical period plasticity in local cortical circuits. *Nat. Rev. Neurosci.* 6:877–888.

Hutson, L.D., and M. Bothwell. 2001. Expression and function of *Xenopus laevis* p75(NTR) suggest evolution of developmental regulatory mechanisms. *J. Neurobiol.* 49:79–98.

Hwang, J.J., M.H. Park, S.Y. Choi, and J.Y. Koh. 2005. Activation of the Trk signaling pathway by extracellular zinc. Role of metalloproteinases. *J. Biol. Chem.* 280:11995–12001.

Ibanez, C.F. 2002. Jekyll-Hyde neurotrophins: the story of proNGF. *Trends Neurosci.* 25:284–286.

Je, H.S., J. Zhou, F. Yang, and B. Lu. 2005. Distinct mechanisms for neurotrophin-3-induced acute and long-term synaptic potentiation. *J. Neurosci.* 25:11719–11729.

Je, H.S., F. Yang, J. Zhou, and B. Lu. 2006. Neurotrophin 3 induces structural and functional modification of synapses through distinct molecular mechanisms. *J. Cell Biol.* 175:1029–1042.

Katz, L.C., and C.J. Shatz. 1996. Synaptic activity and the construction of cortical circuits. *Science*. 274:1133–1138.

Kherif, S., M. Dehaupas, C. Lafuma, M. Fardeau, and H.S. Alameddine. 1998. Matrix metalloproteinases MMP-2 and MMP-9 in denervated muscle and injured nerve. *Neuropathol. Appl. Neurobiol.* 24:309–319.

Korte, M., P. Carroll, E. Wolf, G. Brem, H. Thoenen, and T. Bonhoeffer. 1995. Hippocampal long-term potentiation is impaired in mice lacking brain-derived neurotrophic factor. *Proc. Natl. Acad. Sci. USA*. 92:8856–8860.

Lee, R., P. Kermani, K.K. Teng, and B.L. Hempstead. 2001. Regulation of cell survival by secreted proneurotrophins. *Science*. 294:1945–1948.

Lichtman, J.W., and H. Colman. 2000. Synapse elimination and indelible memory. *Neuron*. 25:269–278.

Lo, Y.J., and M.M. Poo. 1991. Activity-dependent synaptic competition in vitro: heterosynaptic suppression of developing synapses. *Science*. 254:1019–1023.

Lo, Y.J., and M.M. Poo. 1994. Heterosynaptic suppression of developing neuromuscular synapses in culture. *J. Neurosci.* 14:4684–4693.

Lo, Y.J., Y.C. Lin, D.H. Sanes, and M.M. Poo. 1994. Depression of developing neuromuscular synapses induced by repetitive postsynaptic depolarizations. *J. Neurosci.* 14:4694–4704.

Lohof, A.M., N.Y. Ip, and M.M. Poo. 1993. Potentiation of developing neuromuscular synapses by the neurotrophins NT-3 and BDNF. *Nature*. 363: 350–353.

Lu, B. 2003. BDNF and activity-dependent synaptic modulation. *Learn. Mem.* 10:86–98.

Lu, B., and H.S. Je. 2003. Neurotrophic regulation of the development and function of the neuromuscular synapses. *J. Neurocytol.* 32:931–941.

Lu, B., P.T. Pang, and N.H. Woo. 2005. The yin and yang of neurotrophin action. *Nat. Rev. Neurosci.* 6:603–614.

Matsumoto, T., S. Rauskolb, M. Polack, J. Klose, R. Kolbeck, M. Korte, and Y.A. Barde. 2008. Biosynthesis and processing of endogenous BDNF: CNS neurons store and secrete BDNF, not pro-BDNF. *Nat. Neurosci.* 11:131–133.

Nagappan, G., E. Zaitsev, V.V. Senatorov Jr., J. Yang, B.L. Hempstead, and B. Lu. 2009. Control of extracellular cleavage of ProBDNF by high frequency neuronal activity. *Proc. Natl. Acad. Sci. USA*. 106:1267–1272.

Pang, P.T., H.K. Teng, E. Zaitsev, N.T. Woo, K. Sakata, S. Zhen, K.K. Teng, W.H. Yung, B.L. Hempstead, and B. Lu. 2004. Cleavage of proBDNF by tPA/plasmin is essential for long-term hippocampal plasticity. *Science*. 306:487–491.

Patterson, S.L., T. Abel, T.A. Deuel, K.C. Martin, J.C. Rose, and E.R. Kandel. 1996. Recombinant BDNF rescues deficits in basal synaptic transmission and hippocampal LTP in BDNF knockout mice. *Neuron*. 16:1137–1145.

Poo, M.M. 2001. Neurotrophins as synaptic modulators. *Nat. Rev. Neurosci.* 2:24–32.

Rosch, H., R. Schweigreiter, T. Bonhoeffer, Y.A. Barde, and M. Korte. 2005. The neurotrophin receptor p75NTR modulates long-term depression and regulates the expression of AMPA receptor subunits in the hippocampus. *Proc. Natl. Acad. Sci. USA*. 102:7362–7367.

Ryan T.A., H. Reuter, B. Wendland, F.E. Schweizer, R.W. Tsien, and S.J. Smith. 1993. The kinetics of synaptic vesicle recycling measured at single presynaptic boutons. *Neuron*. 11:713–724.

Schoser, B.G., and D. Blottner. 1999. Matrix metalloproteinases MMP-2, MMP-7 and MMP-9 in denervated human muscle. *Neuroreport*. 10:2795–2797.

Taha, S.A., and M.P. Stryker. 2005. Molecular substrates of plasticity in the developing visual cortex. *Prog. Brain Res.* 147:103–114.

Teng, H.K., K.K. Teng, R. Lee, S. Wright, S. Tevar, R.D. Almeida, P. Kermani, R. Torkin, Z.Y. Chen, F.S. Lee, et al. 2005. ProBDNF induces neuronal apoptosis via activation of a receptor complex of p75NTR and sortilin. *J. Neurosci.* 25:5455–5463.

VanSaun, M., and M.J. Werle. 2000. Matrix metalloproteinase-3 removes agrin from synaptic basal lamina. *J. Neurobiol.* 43:140–149.

Walsh, M.K., and J.W. Lichtman. 2003. In vivo time-lapse imaging of synaptic takeover associated with naturally occurring synapse elimination. *Neuron*. 37:67–73.

Wan, J., and M. Poo. 1999. Activity-induced potentiation of developing neuromuscular synapses. *Science*. 285:1725–1728.

Wang, T., K.W. Xie, and B. Lu. 1995. Neurotrophins promote maturation of developing neuromuscular synapses. *J. Neurosci.* 15:4796–4805.

Woo, N.H., H.K. Teng, C.J. Siao, C. Chiaruttini, P.T. Pang, T.A. Milner, B.L. Hempstead, and B. Lu. 2005. Activation of p75NTR by proBDNF facilitates hippocampal long-term depression. *Nat. Neurosci.* 8:1069–1077.

Xie, K., T. Wang, P. Olafsson, K. Mizuno, and B. Lu. 1997. Activity-dependent expression of NT-3 in muscle cells in culture: implications in the development of neuromuscular junctions. *J. Neurosci.* 17:2947–2958.

Yan, Q., and E.M. Johnson Jr. 1988. An immunohistochemical study of the nerve growth factor receptor in developing rats. *J. Neurosci.* 8:3481–3498.

Yang, F., X. He, L. Feng, K. Mizuno, X.W. Liu, J. Russell, W.C. Xiong, and B. Lu. 2001. PI-3 kinase and IP3 are both necessary and sufficient to mediate NT3-induced synaptic potentiation. *Nat. Neurosci.* 4:19–28.

Yang, J., C.J. Siao, G. Nagappan, T. Marinic, D. Jing, K. McGrath, Z.Y. Chen, W. Mark, L. Tessarollo, F.S. Lee, et al. 2009. Neuronal release of proBDNF. *Nat. Neurosci.* 12:113–115.

Yuan, X.B., M. Jin, X. Xu, Y.Q. Song, C.P. Wu, M.M. Poo, and S. Duan. 2003. Signalling and crosstalk of Rho GTPases in mediating axon guidance. *Nat. Cell Biol.* 5:38–45.